ELSEVIER

Preparation and electrochemical properties of SAM of alkanethiols functionalized with 2-aza[3]ferrocenophane on gold electrode

Masaki Horie [*],[1], Tatsuaki Sakano, Kohtaro Osakada

Chemical Resources Laboratory, Tokyo Institute of Technology, 4259 Nagatsuta, Midori-ku, Yokohama 226-8503, Japan

Abstract

Thiols functionalized with *N*-aryl[3]azaferrocenophane formulated as $HS\text{-}(CH_2)_n\text{-}N(CH_2Cp)_2Fe$ (**1**: $n = 6$, **2**: $n = 8$, **3**: $n = 10$, **4**: $n = 12$) and disulfide obtained by oxidation of **4** (**5**) were synthesized via three or four steps reactions starting from 1,1′-ferrocenedimethanol, 4-aminophenol, and α,ω-aklanedithiol. Self-assembled monolayers (SAMs) of these thiols and disulfide on gold electrode were prepared by immersing the electrode in MeCN solutions of the compounds. Cyclic voltammograms of the SAM of **1** ($n = 6$) exhibited reversible redox of the Fe center at $E_{1/2} = 0.26$ V (vs. Ag^+/Ag) in the presence of Et_4NBF_4 in MeCN and at $E_{1/2} = 0.40$ V (vs. AgCl/Ag) in the presence of $NaClO_4$ in H_2O. Addition of $HClO_4$ to the solutions shifted the redox peaks to higher potentials, $E_{1/2} = 0.51$ V (vs. Ag^+/Ag) in MeCN and $E_{1/2} = 0.48$ V (vs. AgCl/Ag) in H_2O, respectively, which was ascribed to positive charge of tertiary ammonium group formed by protonation of the amino group of the azaferrocenophane. $E_{1/2}$ of SAM of **1** in H_2O solution varies depending on the anion contained in the electrolyte, $NaClO_4$ (0.40 V), $NaBF_4$ (0.46 V), Na_2SO_4 (0.53 V), and NaCl (0.55 V). Kinetic data of electron transfer between the Fe center and the gold surface of the SAM of **2**–**4** were obtained with variable scanning rate. Laviron's analysis provided tunneling constant β, 0.05 Å^{-1}, suggesting that the structural changes in the SAMs on oxidation/reduction undergoes the insignificant change of the kinetic constants of the electron transfer depending on the range of the spacer length. In the acidic aqueous media, the kinetic parameters indicated that the imbalanced electron transfer between oxidized and reduced states of the Fe center was caused by the protonation of bridged amine group of azaferrocenophane.
© 2006 Elsevier B.V. All rights reserved.

Keywords: Azaferrocenophane; Self-assembled monolayer; Electrochemistry; Electron transfer

1. Introduction

Alkanethiols form stable self-assembled monolayers (SAMs) on surface of gold, which provides attractive two dimensional aggregates of the compounds [1,2]. SAMs of ferrocene-containing thiols [3] have widely been investigated because they contain redox active ferrocene moiety in addition to the long alkyl [4] or π-conjugated [5] car-rier-tunneling chain and a mercapto group that fixes the organic molecule on the metal electrode surface. Introduction of various functional groups to the cyclopentadienyl (Cp) ligand changes electronic state of the ferrocenyl group and electrochemical response of the SAM electrodes that contain ferrocenyl groups [6]. Previous studies on kinetics [7,8] and thermodynamics of electron transfer of the SAMs have revealed that the redox potential between neutral Fe(II) state and cationic Fe(III) state is tuned by changing the structures of the functionalized organic or organometallic [9] compounds.

We reported recently Ru catalyzed condensation [10] of 1,1′-bis(hydroxymethyl)ferrocene with primary amines to produce *N*-aryl (or alkyl)-2-aza[3]ferrocenophanes [11].

---
[*] Corresponding author. Tel.: +81 48 467 9146; fax: +81 48 467 9389.
E-mail address: mhorie@riken.jp (M. Horie).
[1] Present address: Supramolecular Science Laboratory, RIKEN (The Institute of Physical and Chemical Research), 2-1 Hirosawa, Wako, Saitama 351-0198, Japan.
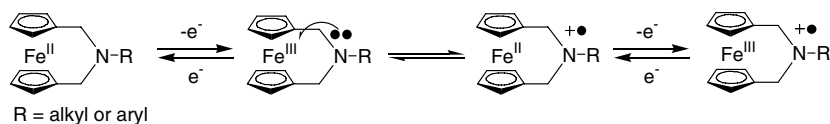
Scheme 1.

The 2-aza[3]ferrocenophanes show multi-step redox, which includes oxidation and reduction of Fe center, rapid and reversible electron transfer between the Fe and N atoms at the oxidized state, and further oxidation of the one electron oxidized species, as shown in Scheme 1. This electronic communication between the Fe center and nitrogen atom of the ligand accelerates the thermal isomerization of *cis*-azobenzene group to *trans*-structure in the ligand [12], or induces formal protonation of the amino group in the presence of a hydrogen radical source [13].

Fixation of 2-aza[3]ferrocenophanes on the metal surface will provide the electrode functionalized by the organometallic group which exhibits the multi-step redox or oxidation of the organic group induced by redox of the Fe center. In this paper, we report preparation of a new type of 2-aza[3]ferrocenophanes formulated as HS-$(CH_2)_n$-N$(CH_2Cp)_2$Fe (**1**: $n = 6$, **2**: $n = 8$, **3**: $n = 10$, **4**: $n = 12$) and disulfide of **4** (**5**) and the electrochemical properties of their SAMs formed on gold surface.

2. Results and discussion

2.1. Synthesis and characterization of azaferrocenophanes

Scheme 2 summarizes the synthesis of alkanethiol and functionalized by 2-aza[3]ferrocenophane dialkyldisulfide. Reactions of *N*-(4-hydroxyphenyl)-2-aza[3]ferrocenophane with α,ω-dibromoalkane, Br$(CH_2)_n$Br ($n = 6, 8, 10, 12$), in

the presence of NaH produce the corresponding bromoalkoxy-2-aza[3]ferrocenophanes in 45–69% yields. The products react with thiourea to give the corresponding mercaptoalkoxy-2-aza[3]ferrocenophanes **1**–**4** in 56–68% yields. Oxidation of **4** under air affords the corresponding disulfide **5**. The ^{1}H NMR spectra of **1**–**4** exhibit the signals of –CH$_2$SH group at δ 2.53–2.55 (–CH$_2$–) and 1.34–1.37 (–SH), while the signal of –CH$_2$SS– hydrogen of **5** is observed at δ 2.69 (Fig. 1).

2.2. Electrochemical properties of SAMs of azaferrocenophanes

The SAMs on gold surface were prepared by immersion of gold electrode in a MeCN solution containing **1**–**4** (0.10 mM) and **5** (0.05 mM), respectively, for 12 h, and rinsing with absolute MeCN and then with distilled water.
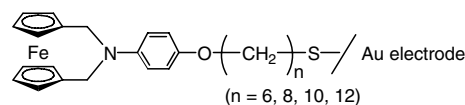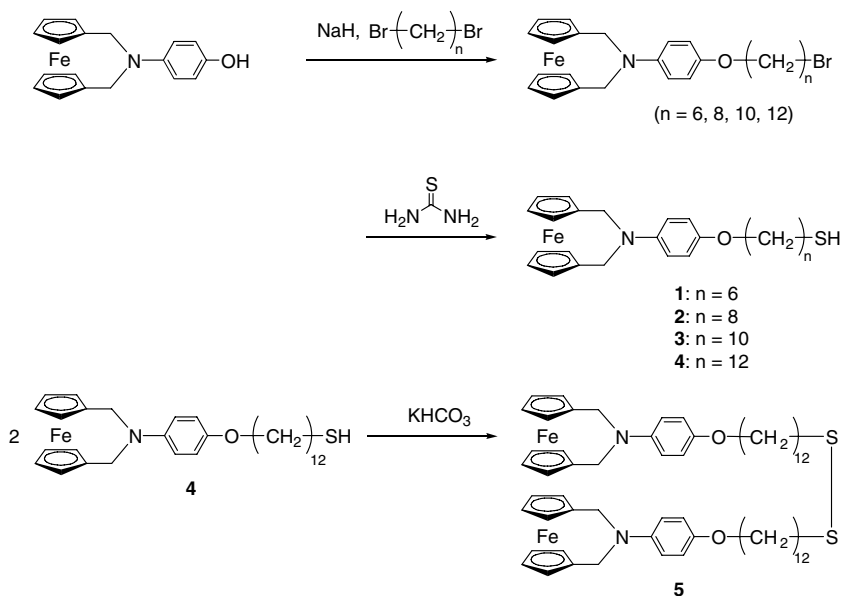

Fig. 2a shows cyclic voltammogram of SAM of **1** in MeCN solution of Et$_4$NBF$_4$ (0.10 M) with a scan rate of 0.10 V s^{-1}. A reversible redox peak pair of Fe(III)/Fe(II) of the azaferrocenophane group is observed at $E_{pa} = 0.27$ V and $E_{pc} = 0.24$ V (vs. Ag$^+$/Ag). The peak sep-

Scheme 2. Synthesis of 2-aza[3]ferrocenophane tethered to alkanethiol and its disulfide.
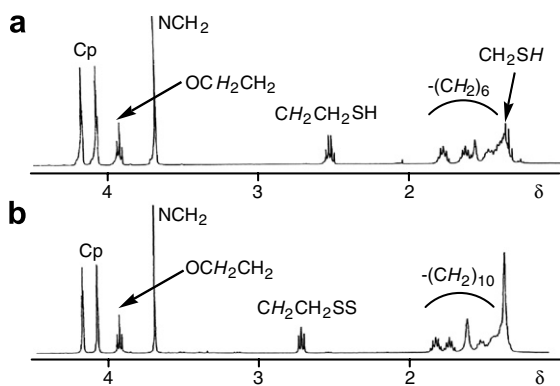
Fig. 1. ^{1}H NMR spectra of (a) **4** and (b) **5** in CDCl$_3$.

aration of SAM of **1**, $\Delta E = E_{pa} - E_{pc} = 0.03$ V, is smaller than that of **1** ($\Delta E = 0.08$ V) and *N*-(4-hydroxyphenyl)-2-aza[3]ferrocenophane ($\Delta E = 0.07$ V) [11] measured in their MeCN solutions, suggesting that electron transfer in Fig. 2a takes place within the SAM. Fig. 2b depicts the cyclic voltammogram of SAM of **1** in MeCN solution of a mixture of Et$_4$NBF$_4$ and HClO$_4$. The redox peaks are shifted to higher potentials, $E_{pa} = 0.53$ V and $E_{pc} = 0.48$ V than those without addition of HClO$_4$. Fig. 3 shows change

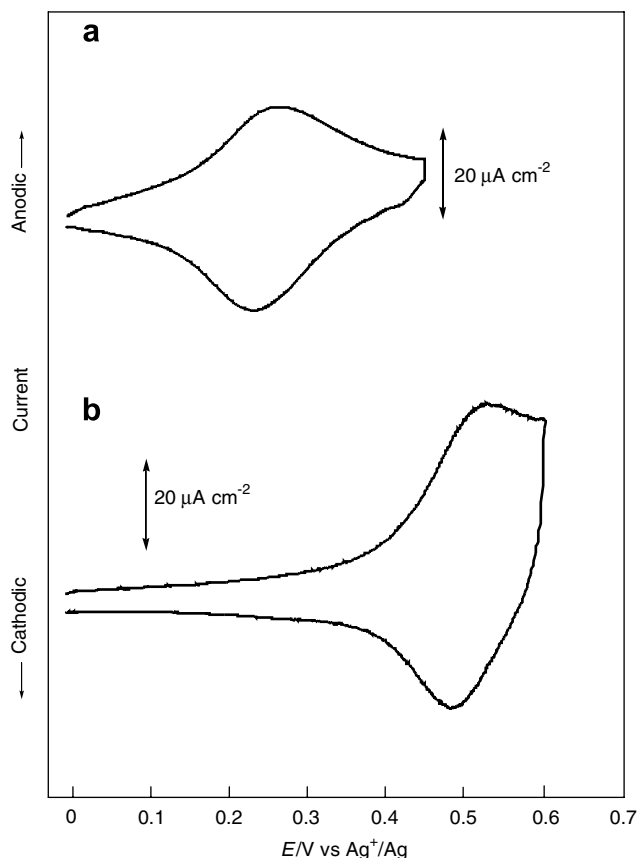of the redox potential caused by change of pH of the solution. Both E_{pa} and E_{pc} of SAM of **1** increases to a great extent by decrease of the pH value in the region with pH < 3.3, while, in the solution with pH > 3.3, the change of $E_{1/2}$ caused by pH change is less significant. This pH dependence of the redox potential is reversible and can be reproduced even after immersing the electrode in acidic and basic aqueous solutions alternatively. Bordwell and co-workers reported acidities of protonated nitrogen compounds, such as *N,N*-dimethyl-4-methoxyanilinium salt (pK_a = 3.6) [14]. These results can be ascribed to protonation of the amine nitrogen of the azaferrocenophane in the low pH region. Addition of HClO$_4$ to the solution causes protonation of the amine nitrogen of the 2-aza[3]ferrocenophane group (Scheme 3), and positive charge of the produced trisubstituted ammonium renders the redox potential of the ferrocene group higher than that without the protonation. Secondary and tertiary amine groups in the aminomethylferrocene were also reported to change the redox potentials upon protonation or alkylation of the nitrogen atom [11–13].

Kaifer and co-workers investigated electrochemical properties of the dendrimers containing two ferrocenyl groups bridged by the aminomethyl group and observed inhibition of electron transfer between the ferrocenyl groups caused by protonation of the nitrogen atom [15]. The ferrocenyl groups of the dendrimer generate mixed valent species upon electrochemical oxidation, while protonation of the bridged aminomethyl group inhibits the electrochemical communication.

Fig. 4a and b shows the cyclic voltammograms of SAM of **4** in 0.10 M NaClO$_4$ aqueous solution and in the solution of NaClO$_4$ and HClO$_4$, respectively. Reversible redox peaks of Fe(III)/Fe(II) of the azaferrocenophane group are

Fig. 2. Cyclic voltammograms of **1** deposited on gold electrode (a) in MeCN containing 0.10 M Et$_4$NBF$_4$ ($E_{pa} = 0.27$ V and $E_{pc} = 0.24$ V) and (b) in MeCN containing 0.10 M Et$_4$NBF$_4$ and HClO$_4$ ($E_{pa} = 0.53$ V and $E_{pc} = 0.48$ V) at 25 °C. Scan rate: 0.10 V s^{-1}.
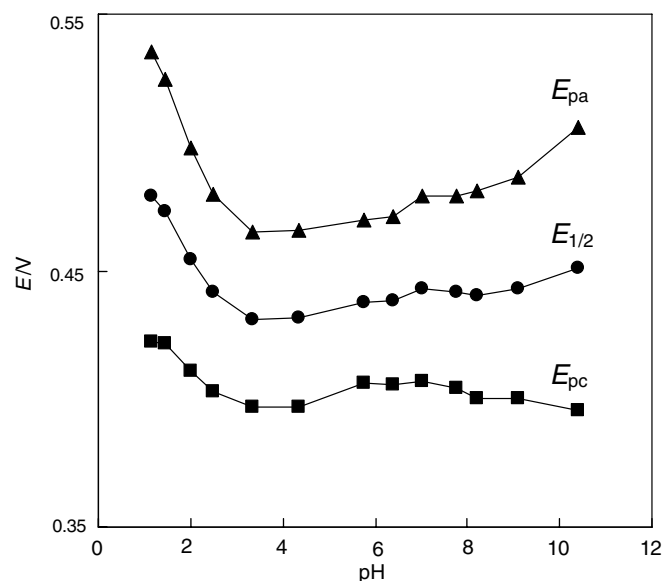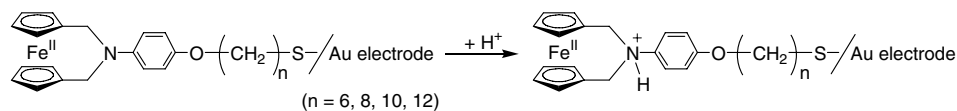

Fig. 3. pH dependence of peak position in SAM of **1** in contact with solutions of a mixture of NaClO$_4$ and HClO$_4$ at 25 °C. The potentials were referenced with AgCl/Ag. Scan rate: 0.1 V s^{-1}.

Scheme 3. The protonation of the amine nitrogen of the azaferrocenophane.

observed at $E_{pa} = 0.48$ V and $E_{pc} = 0.42$ V (vs. Ag$^+$/Ag) at scan rate of 0.10 V s^{-1} in the neutral solution, while the oxidation peak in the solution containing HClO$_4$ is observed at higher potentials at $E_{pa} = 0.56$ V. The shift of the oxidation potential is ascribed to protonation of the amine group of the azaferrocenophane. The peak currents are expressed as Eq. (1), according to Langmuir isotherm equation on electrode surface [16]

$$i_p = n^2 F^2 \Gamma_t v / (4RT) \qquad (1)$$

in which, n, Γ_t, and v, denote the number of electron, total concentration of immobilized molecules, and scan rate, respectively. Fig. 5a and b plots intensities of the anodic and cathodic peaks of SAM of **4** in the solutions of NaClO$_4$ and of NaClO$_4$ and HClO$_4$, respectively. The former solution shows linear relationship between peak currents I_a

or I_c and scan rate v in the range of the scan rate from 0.02 to 12 V s^{-1}. The electron transfer between the electrode and the ferrocenyl group takes place reversibly with the scan rate up to 12 V s^{-1}. On the basis of integration of the voltammetric peak, the density of the electrochemically active ferrocenophane-containing thiol molecules on the surface of the electrode is approximately 9.8×10^{-11} mol cm^{-2}, which corresponds to coverage rates $\Gamma/\Gamma_{max} = 0.21$ [4b,17,18]. Fig. 5b exhibits linear relationship of the intensities of the anodic and cathodic peaks with the scan rate in the range below 5 V s^{-1}. The peaks become broad with increasing scan rate above 5 V s^{-1}. These results indicate the structural change in the SAM in the acidic media. Our previous report shows that the structural change of the azaferrocenophane with the protonation of the nitrogen atom [19]. The variety of the surface structures are provided by the protonation of the nitrogen atom of the aza-

Fig. 4. Cyclic voltammograms of **4** deposited on gold electrode (a) in aqueous media containing 0.10 M NaClO$_4$ ($E_{pa} = 0.48$ V and $E_{pc} = 0.42$ V) and (b) in acidic aqueous media containing 0.10 M HClO$_4$ ($E_{pa} = 0.56$ V and $E_{pc} = 0.42$ V) at 25 °C. Scan rate: 0.10 V s^{-1}.

Fig. 5. Dependence on scan rate of I_p of cyclic voltammogram in SAM of **4** (a) in contact with aqueous solution of 0.10 M NaClO$_4$ and (b) with acidic aqueous solution containing 0.10 M HClO$_4$. Anodic peak I_{pa} and cathodic peak I_{pc} are shown.
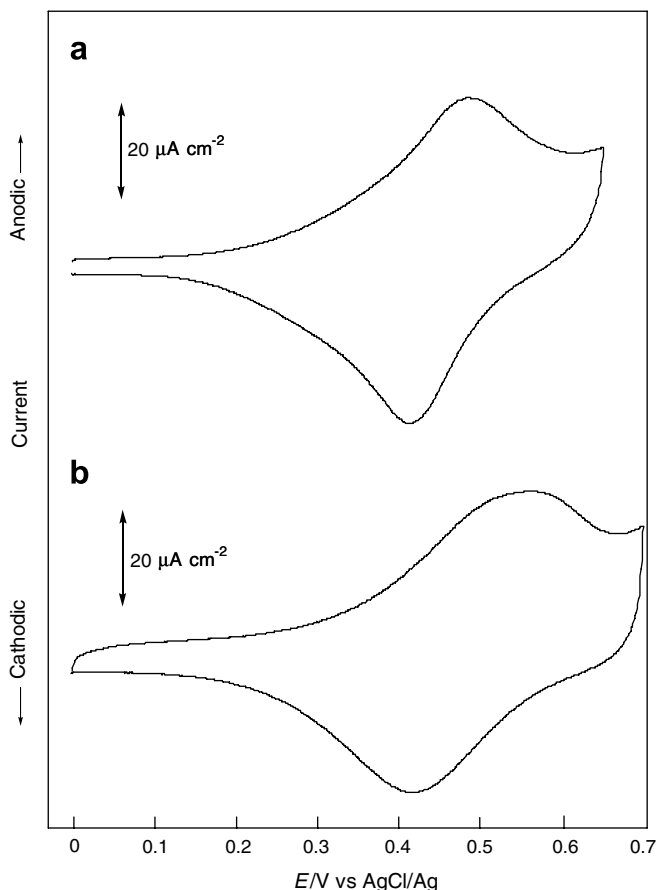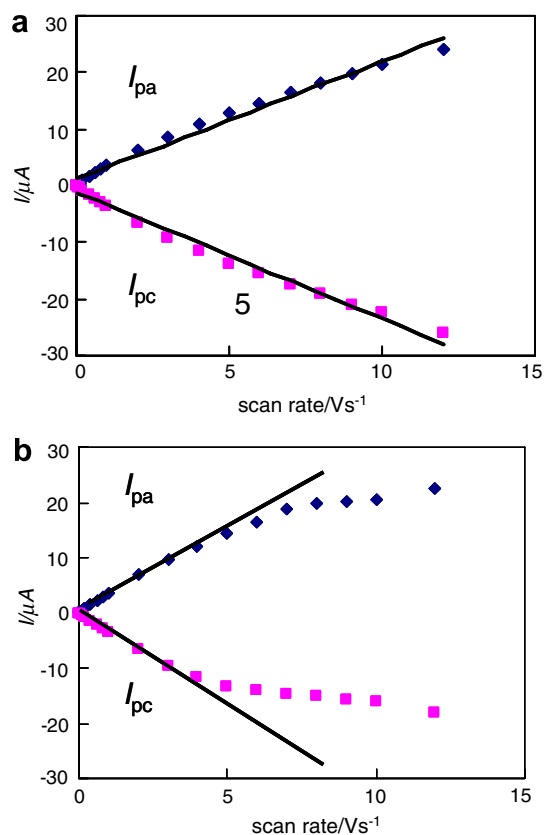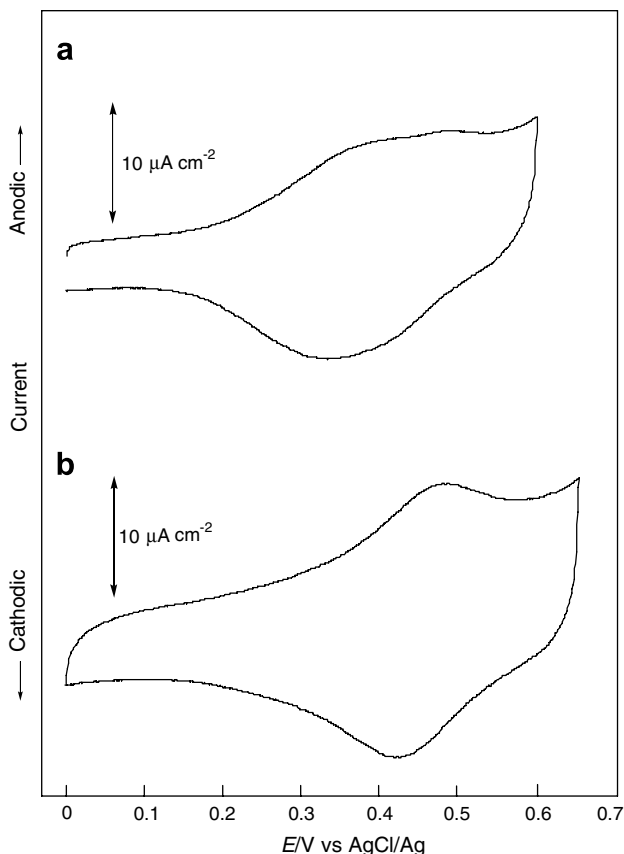
Fig. 6. Cyclic voltammograms of **5** deposited on gold electrode (a) in aqueous media containing 0.10 M NaClO$_4$ (E_{pa} = 0.41 V, 0.49 V and E_{pc} = 0.33 V) and (b) in acidic aqueous media containing 0.10 M HClO$_4$ (E_{pa} = 0.48 V and E_{pc} = 0.42 V) at 25 °C. Scan rate: 0.10 V s^{-1}.

Fig. 7. Cyclic voltammograms of mixed SAM of (a) **4** (E_{pa} = 0.21 V and E_{pc} = 0.08 V) and (b) **5** (E_{pa} = 0.22 V and E_{pc} = 0.04 V) in aqueous media containing 0.10 M NaClO$_4$ at 25 °C. Scan rate: 0.10 V s^{-1}.

ferrocenophane because of the fixation of the azaferrocenophane on the gold surface.

Disulfide **5** contains the two azaferrocenophane groups tethered by (CH$_2$)$_{12}$–S–S–(CH$_2$)$_{12}$ chain. As shown in Fig. 6a, the cyclic voltammogram of SAM exhibits the two anodic peaks at E_{pa} = 0.41, 0.49 V and a cathodic peak at E_{pc} = 0.33 V in the neutral aqueous media, and the peaks of the voltammogram in acidic aqueous media are observed at E_{pa} = 0.48 V and E_{pc} = 0.42 V, as shown in Fig. 6b. The multiple oxidation peaks may suggest the presence of Fe centers which are close positions to each other and undergo electrochemical interaction between them, although irregular absorption of the disulfide on the metal surface might also cause such disorder of the electrochemical behavior [20]. The intermolecular interaction of **5** is small in SAM, because the coverage of SAM of **5** (Γ/Γ_{max} = 0.074) is smaller than SAM of **4** (Γ/Γ_{max} = 0.21). We prepared mixed SAMs of **4** and of **5** with dodecanethiol on gold electrode in order to compare the electrochemical properties with SAMs composed of the ferrocenophane-containing thiols or disulfide only. Dodecanethiol is expected to form the mixed SAMs suitable for this study because it has sufficient length of the oligo-methylene chain to make stable SAM and to prevent the thiol with 2-aza[3]ferrocenophane group from intermolecular electro-
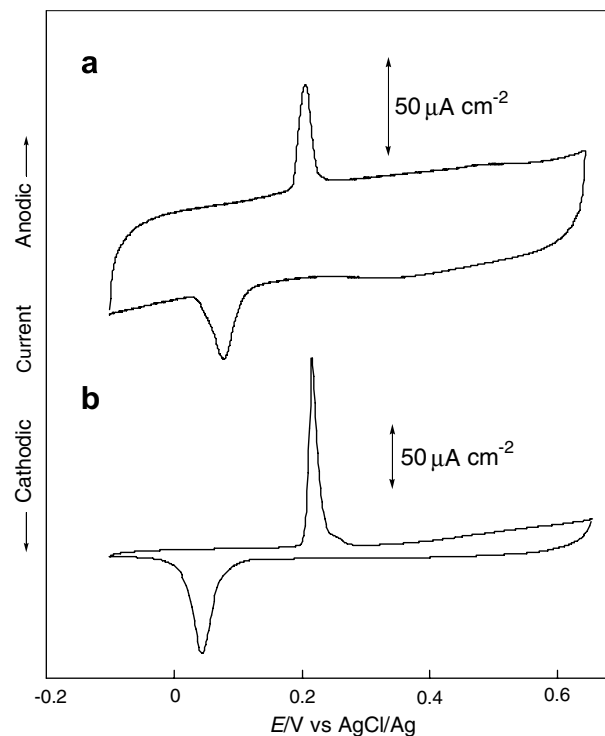
chemical interaction. The mixed SAM of **4** with dodecanethiol is constructed by dipping the Au electrode in a MeCN solution of a mixture of **4** (0.10 mM) and dodecanethiol (0.10 mM). As shown in Fig. 7a, the cyclic voltammogram of mixed SAM prepared from **4** and dodecanethiol in H$_2$O exhibits a pair of the sharp peaks at E_{pa} = 0.21 V and E_{pc} = 0.08 V; the full width at half maximum (FWHM) values are estimated to be 0.024 V for anodic and to be 0.038 V for cathodic, respectively. These results show formation of the mixed SAM without irregularities of the assembly of the molecules on gold surface. Uosaki and co-workers reported the cyclic voltammogram of the gold electrode modified with a monolayer of 6-ferrocenylhexanethiol, which showed very sharp redox peaks (FWHM = 21 mV) [21]. They attributed the spikes to the quality of the monolayer. Large peak-to-peak separation ($\Delta E = E_{pc} - E_{pa}$ = 0.13 V) suggests a slower electron transfer reaction between the Fe center and the gold surface than the SAMs composed of **4** and **5** only (Figs. 4a and 6a). The mixed SAMs of the mercaptooctylhydroquinone with alkanethiols was reported to show similar large peak separation because dense alignment of alkanethiols blocks the direct electron transfer between the redox active hydroquinone or quinine sites and metal surface [22]. As shown in Fig. 7b, the voltammogram of the mixed SAM prepared from disulfide **5** and dodecanethiol shows a similar redox to the mixed SAM of **4** with a small potential width, and its FWHM is estimated to 0.015 V for anodic peak and 0.032 V for cathodic. Thus, the two oxidation

Table 1
Electrochemical data of SAMs[a]

Thiol (mM)	Media	$HClO_4$ (M)	E_{pa} (V)	E_{pc} (V)	$E_{1/2}$ (V)[b]	$\Gamma \times 10^{-10}$ (mol cm^{-2})	Γ/Γ_{max}[c]
1 (0.10)	MeCN	0	0.27[d]	0.24[d]	0.26 (0.03)[d]	0.68	0.15
1 (0.10)	MeCN	0.10	0.53[d]	0.48[d]	0.51 (0.05)[d]	0.68	0.15
1 (0.10)	H_2O	0	0.46	0.34	0.40 (0.12)	1.5	0.33
1 (0.10)	H_2O	0.10	0.55	0.41	0.48 (0.14)	1.5	0.33
2 (0.10)	H_2O	0	0.48	0.40	0.44 (0.08)	0.60	0.13
2 (0.10)	H_2O	0.10	0.52	0.41	0.47 (0.11)	0.60	0.13
3 (0.10)	H_2O	0	0.49	0.41	0.45 (0.08)	0.82	0.18
3 (0.10)	H_2O	0.10	0.54	0.44	0.49 (0.10)	0.82	0.18
4 (0.10)	H_2O	0	0.48	0.42	0.45 (0.06)	0.98	0.21
4 (0.10)	H_2O	0.10	0.56	0.42	0.49 (0.14)	0.98	0.21
4 (0.10)[e]	H_2O	0	0.21	0.08	0.15 (0.13)	0.017	0.0037
5 (0.05)	H_2O	0	0.41, 0.49	0.33	0.37 (0.08)	0.34	0.074
5 (0.05)	H_2O	0.10	0.48	0.42	0.45 (0.06)	0.34	0.074
5 (0.05)[e]	H_2O	0	0.22	0.04	0.13 (0.18)	0.18	0.039
5 (0.05)[f]	H_2O	0	0.24	0.00	0.12 (0.24)	0.020	0.0043

[a] All measurements were performed at 25 °C. Each solution contains 0.10 M Et_4NBF_4 (in CH_3CN) or 0.10 M $NaClO_4$ (in H_2O) as the electrolyte. The potentials were recorded to AgCl/Ag.
[b] ΔE ($E_{pa} - E_{pc}$, V) is shown in parentheses.
[c] Maximum coverage of ferrocene, $\Gamma_{max} = 4.6 \times 10^{-10}$ mol cm^{-2} reported on previous literature [4b,17,18].
[d] The potentials were recorded to Ag^+/Ag in MeCN solution.
[e] The electrodes modified mixed SAM were prepared by immersing of gold electrode into the solution of the mixture of the azaferrocenophanes and n-$C_{12}H_{25}SH$ (0.10 M).
[f] Analogous method of e, however, n-$C_{12}H_{25}SH$ (1.0 M).

peaks in SAM of **5** (Fig. 6a) is ascribed to the presence of ferrocenophane groups with different circumstances rather than to the electrochemical interaction between the ferrocenophane groups situated at close positions to each other.

Table 1 summarizes the electrochemical data of SAMs of **1**–**5** and the mixed SAMs with dodecanethiol. All SAMs show the redox pair of azaferrocenophane moiety, and Γ/Γ_{max} are estimated to 0.13–0.33 (SAMs **1**–**4**) and 0.074 (SAM **5**), while the mixed SAMs with dodecanethiol provide much smaller Γ/Γ_{max} (0.0037 for **4** and 0.0043 for **5**). In the neutral aqueous media, $E_{1/2}$ increases with increase of the carbon number of the alkylene chain spacer. The electrochemical oxidation of the azaferrocenophane-containing thiol with longer alkylene spacer occurs at higher potential in the neutral media. On the other hand, in the acidic media, the redox potentials of the azaferrocenophane moiety of all SAMs shift to higher potentials (SAM **1**–**4**; $E_{1/2} = 0.47$–0.49 V) by protonation of the amine part of the azaferrocenophanes, and the potentials do not vary depending on the length of the alkyl chain spacer. Thus, it is suggested that the length of alkylene chain spacer governs the electron transfer between the azaferrocenophane moiety and gold surface in the neutral media, while the trialkyl ammonium group formed by protonation forms a significant barrier for the electron transfer in the acidic media.

Table 2 summarizes the redox potentials of SAM of **1** measured in aqueous solutions that contain various electrolytes. Position of the anodic peak potentials, E_{pa}, varies depending on the kind of anions of the electrolyte. E_{pa} values are shifted to higher potential in the order of the anions; ClO_4^- (0.46 V vs. AgCl/Ag), BF_4^- (0.50 V), Cl^- (0.61 V), and SO_4^{2-} (0.69 V). Such a behavior was observed

also in the former studies on ferrocene-terminated SAMs, and the results are attributed to degree of hydrophilicity of the anions, in the order of $ClO_4^- > BF_4^- > Cl^- > SO_4^{2-}$ [23]. Table 2 lists FWHM of the electrochemical reaction which increases by the anions in the order of $ClO_4^- < BF_4^- < Cl^- < SO_4^{2-}$. The hydrophobic ClO_4^- anion easily penetrates into the redox active surface to produce a strong ion pair with the ferrocenium cation during the oxidation, and the produced ion pair stabilizes the redox active surface without lateral repulsion of the ferrocene moiety and decreases the FWHM. On the other hand, the most hydrophilic SO_4^{2-} anion and small Cl^- anion tend to be located outside the SAM with increasing lateral repulsive interactions between the redox active moieties to increase FWHM [23c].

2.3. Kinetic data of SAMs of azaferrocenophanes

Kinetic data of electron transfer between the Fe center and the gold surface of the SAM of **2**–**4** are obtained with

Table 2
Summary of redox potentials of SAM of **1** in various solutions[a]

Electrolyte	E_{pa} (V)	E_{pc} (V)	$E_{1/2}$ (V)	FWHM (V)[b]
$NaClO_4$	0.46	0.34	0.40	0.08
$NaBF_4$	0.50	0.41	0.46	0.12
NaCl	0.61	0.49	0.55	0.13
Na_2SO_4	0.69	0.37	0.53	0.22
$HClO_4$	0.55	0.42	0.49	0.12

[a] All measurements were performed in H_2O containing 0.2 M of electrolyte at 25 °C. The potentials were recorded to AgCl/Ag. Scan rate: 0.10 V s^{-1}.
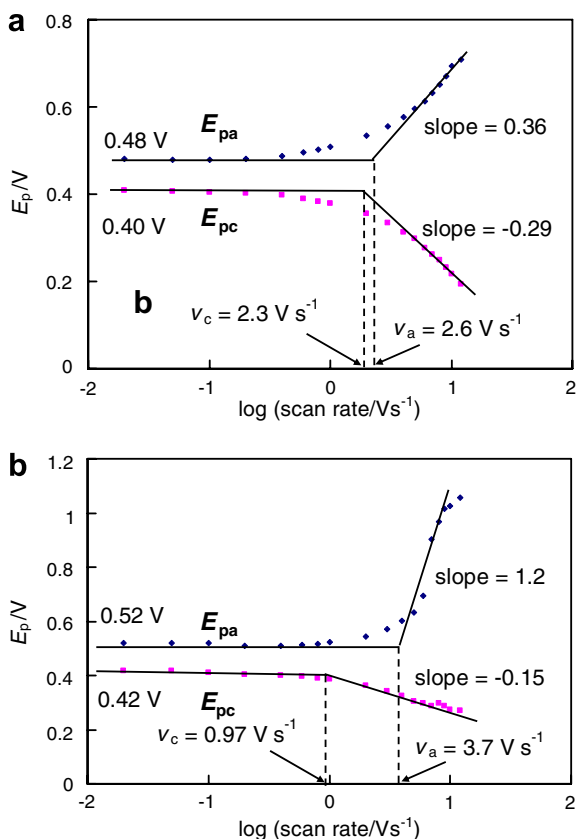[b] Full width at half maximum (FWHM) observed for cathodic peak.

Fig. 8. Dependence on scan rate of E_p of cyclic voltammogram in SAM of **2** (a) in contact with aqueous solution of 0.10 M NaClO$_4$ and (b) with acidic aqueous solution of 0.10 M HClO$_4$. Anodic peak E_{pa} and cathodic peak E_{pc} are shown. The potentials are referenced with AgCl/Ag.

scan rate in the range, 0.02 to 12 V s^{-1}. The SAM of **2** shows quasi-reversible behavior with the scan rate of 0.1–1.0 V s^{-1}, and the peak potential separation significantly increases above 1.0 V s^{-1}. These parameters of the separation are employed to estimate the electron transfer coefficients and the symmetry factors by using Laviron's procedure [7–9]. Fig. 8a shows plots of E_{pa} and E_{pc} vs. log (scan rate/V s^{-1}) for SAM of **2** obtained in neutral aqueous media. From the slope of the plots at high potential regions, the transfer coefficients α and $1 - \alpha$ were calculated as 0.16 and 0.20. They are deviated from 0.5 due to defect of the orientation of the azaferrocenophane-containing molecules on the electrode surface [9,24]. The k values for the anodic and cathodic processes are estimated to 17 and 18 s^{-1}, respectively, and the values are in reasonable agreement with those in the previous reports which showed the rate coefficients in the electron transfer between the electrode and SAM surface through the alkyl spacer [4].

Since dependence of the peak potentials and currents on the scan rate differs between the neutral and acidic media, the kinetic parameters in the acidic media are expected to differ from that in the neutral media. Fig. 8b plots E_{pa} and E_{pc} vs. log of scan rate for SAM of **2** in acidic aqueous media. Separation of the potential is obviously unsymmetrical between anodic and cathodic due to imbalanced mass

transfer abilities of cation and anion included in the electrolyte. The transfer coefficients are estimated to $\alpha = 0.052$ and $1 - \alpha = 0.29$, respectively, and the transfer coefficients are too low to be appropriate for the Laviron procedure. One possible explanation is that the SAMs consist of ferrocene groups having a continuum of rate constants. The anodic peak potentials are influenced by scan rate more significantly than the cathodic ones. The anodic electron transfer rate constant k_a expects to be smaller than the cathodic k_c in the acidic media, while k_a (17 s^{-1}) and k_c (18 s^{-1}) in the neutral media are similar to each other. The stable ion pair composed of the ammonium cation and ClO$_4^-$ is formed in the acidic media and it inhibits further smooth penetration of ClO$_4^-$ into the SAM caused by electrostatic and steric repulsion. It has been reported that the ferrocene-containing SAM forms the stable surface structures by filling the free space with the bulky ClO$_4^-$ anion which has low mass transfer ability [23,25].

Fig. 9 depicts the plots of $\ln k$ vs. length of the calculated spacer between Fe center and gold surface, d, which length were estimated by the ideal molecular models of the azaferrocenophanes, in the neutral aqueous media. The slope of the plots in the neutral media leads to the tunneling constant, $\beta = 0.05$ Å^{-1}, approximately. The electron transfer rate constant of SAM of **2** is decrease with increase of the length of polymethylene spacers. The β calculated from SAMs of **2**–**4** is smaller than that of previous reports (0.5–1.4 Å^{-1}) [4,5,9,22], suggesting that the structural changes in the SAMs on oxidation/reduction undergoes the insignificant change of the kinetic constants of the electron transfer depending on the range of the spacer length ($d = 20.6$–26.2 Å).

Scheme 4 depicts the schematic illustration to account for the electrochemical reactions of the SAM of 2-aza[2]ferrocenophane-containing alkyl thiol. In the neutral media, the electron transfer between the Fe center and the gold surface takes place smoothly, and the rate-determining step consists in the electron-tunneling through the polymethylene spacer of the thiol. On the other hand, in the acidic
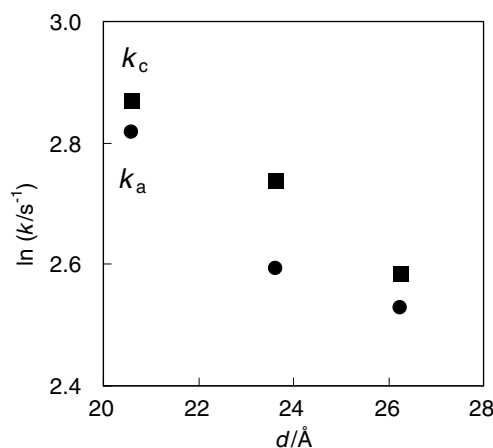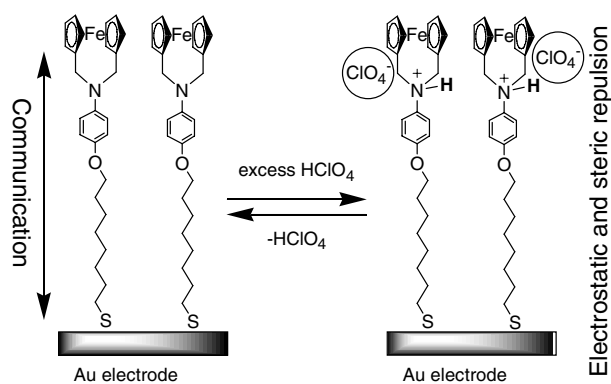

Fig. 9. Plots of $\ln k$ vs. d for anodic (circle) and cathodic (square) in H$_2$O containing 0.10 M NaClO$_4$.

Scheme 4. Schematic illustration of SAM of **4**.

media, protonation of bridged amine of azaferrocenophane shifts the redox peaks to higher potentials than that of neutral media, probably because the produced ammonium cation inhibits smooth electron transfer between the Fe center and the nitrogen atom [11–13]. The imbalanced redox responses of the peak potentials are observed in the acidic media, because of the slow penetration and fast dissociation of ClO_4^- anion due to the electrostatic and steric repulsion between the anions in the redox process.

3. Experimental

3.1. General remarks

All the manipulations of the air-unstable complexes were carried out under nitrogen or argon using standard Schlenk techniques. *N*-(4-Hydroxyphenyl)-2-aza[3]ferrocenophane was prepared according to the literature method [11]. ^{1}H and ^{13}C{^{1}H} NMR spectra were recorded on JEOL EX-400 spectrometers where the chemical shifts were referenced with respect to $CHCl_3$ (δ 7.24) for ^{1}H and $CDCl_3$ (δ 77.0) for ^{13}C as internal standards. Elemental analyses were carried out with a Yanaco MT-5 CHN autorecorder. Cyclic voltammetry (CV) was measured in MeCN containing 0.10 M Et_4NBF_4 or in H_2O containing 0.10 M $NaClO_4$ with ALS Electrochemical Analyzer Model-600A. The measurement was carried out in a standard one-compartment three-electrode cell (10 cm^3) under inert gas equipped with Ag^+/Ag (in nonaqueous media) or AgCl/Ag (in aqueous media) reference electrode, a platinum-wire counter electrode, and a gold-disk working electrode (ID: 1.6 mm). The real surface area of the working electrode was estimated from the integration of the gold surface reduction charge of 8.32 μC at 0.78 V vs. AgCl/Ag. The effective area of the working electrode was estimated to 0.0173 cm^2, which was given by multiple the reduction charge by theoretical charge of 482 μC cm^{-2} [17]. Buffers titrisol were purchased from Kanto Chemical Co., Inc.: pH 1.0; glycine/hydrochloric acid, pH 2.0–4.0; citrate/hydrochloric acid, pH 5.0–6.0; citrate/sodium hydroxide, pH 7.0; phosphate, pH 8.0; borate/hydrochloric acid, pH 9.0–11.0; boric acid/potassium chloride/sodium

hydroxide. TOA Corporation HM-40V pH meter was used for pH measurements.

3.2. Synthesis of N-{4-(6-bromohexyloxy)phenyl}-2-aza[3]ferrocenophane

NaH (0.045 g, 1.88 mmol) was added to a dimethylformamide solution (10 mL) of *N*-(4-hydroxyphenyl)-2-aza[3]ferrocenophane [11] (0.50 g, 1.57 mmol). After stirring at 25 °C for 1 h, 1,6-dibromohexane (3,61 g, 15.7 mmol) was added and the solution was stirred at 50 °C for 24 h. To the reaction mixture was added water, and the product was extracted with chloroform. After the organic layer was dried over Na_2SO_4, the solvent was removed by evaporation to give a yellow powder, which was purified by silica gel column chromatography (eluent = hexane). The solvent was removed by evaporation and the resulting powder was dried in vacuo to give *N*-{4-(6-bromohexyloxy)phenyl}-2-aza[3]ferrocenophane as a yellow solid (0.36 g, 47%). ^{1}H NMR (400 MHz, $CDCl_3$, 25 °C) δ 6.97, 6.85 (d, 4 H, Ph, *J* = 9 Hz), 4.18, 4.08 (d, 8 H, Cp), 3.94 (t, 2H, OCH_2, *J* = 6 Hz), 3.69 (s, 4H, N-CH_2), 3.43 (t, 2H, BrCH_2, *J* = 7 Hz), 1.91 (quintet, 2H, OCH_2CH_2, *J* = 7 Hz), 1.79 (quintet, 2H, BrCH_2CH_2, *J* = 7 Hz), 1.51–1.58 (4H, –(CH_2)–).

Other 2-aza[3]ferrocenophanes having bromoalkyl chain were prepared analogously and their data are shown below.

3.3. N-{4-(8-Bromooctyloxy)phenyl}-2-aza[3]ferrocenophane

Yellow powder (0.38 g, 47%). ^{1}H NMR (400 MHz, $CDCl_3$, 25 °C) δ 6.96, 6.86 (d, 4H, Ph, *J* = 9 Hz), 4.18, 4.08 (d, 8H, Cp), 3.93 (t, 2H, OCH_2, *J* = 6 Hz), 3.69 (s, 4H, N-CH_2), 3.42 (t, 2H, BrCH_2, *J* = 7 Hz), 1.88 (quintet, 2H, OCH_2CH_2, *J* = 7 Hz), 1.78 (quintet, 2H, BrCH_2CH_2, *J* = 7 Hz), 1.26–1.56 (8H, –(CH_2)–). ^{13}C{^{1}H} NMR (100 MHz, in $CDCl_3$ at 25 °C) δ 152.4 (*ipso*, $C_6H_4OCH_2$), 145.1 (*ipso*, C_6H_4N), 117.6 (*meta*, $C_6H_4OCH_2$), 115.5 (*ortho*, $C_6H_4OCH_2$), 84.4 (N-CH_2), 69.9, 69.2 (Cp), 68.5 ($C_6H_4OCH_2$), 48.7 (Cp-CH_2-N), 33.9 ($C_6H_4OCH_2CH_2$), 32.8 (CH_2Br), 29.4, 29.2, 28.7, 28.1, 26.0. Anal. Calc. for $C_{26}H_{32}BrFeNO$: C, 61.20; H, 6.32; N, 2.74; Br, 15.66. Found: C, 60.70; H, 6.17; N, 2.57; Br, 15.99%.

3.4. N-{4-(10-Bromodecyloxy)phenyl}-2-aza[3]ferrocenophane

Yellow powder (0.38 g, 45%). ^{1}H NMR (400 MHz, $CDCl_3$, 25 °C) δ 6.97, 6.85 (d, 4H, Ph, *J* = 9 Hz), 4.18, 4.08 (d, 8H, Cp), 3.93 (t, 2H, OCH_2, *J* = 6 Hz), 3.69 (s, 4H, N-CH_2), 3.41 (t, 2H, BrCH_2, *J* = 7 Hz), 1.86 (quintet, 2H, OCH_2CH_2, *J* = 7 Hz), 1.77 (quintet, 2H, BrCH_2CH_2, *J* = 7 Hz), 1.21–1.50 (12H, –(CH_2)–). ^{13}C{^{1}H} NMR (100 MHz, in $CDCl_3$ at 25 °C) δ 152.3 (*ipso*, $C_6H_4OCH_2$), 144.9 (*ipso*, C_6H_4N), 117.5 (*meta*, $C_6H_4OCH_2$), 115.4 (*ortho*, $C_6H_4OCH_2$), 84.4 (N-CH_2), 69.9, 69.1 (Cp), 68.5

($C_6H_4OCH_2$), 48.6 (Cp-CH_2-N), 34.1 ($C_6H_4OCH_2CH_2$), 32.8 (CH_2Br), 29.5–29.2, 28.7, 28.2, 26.1. Anal. Calc. for $C_{28}H_{36}BrFeNO$: C, 62.47; H, 6.74; N, 2.60; Br, 14.84. Found: C, 62.64; H, 6.43; N, 2.55; Br, 14.87%.

3.5. N-{4-(12-Bromododecyloxy)phenyl}-2-aza[3]ferrocenophane

Yellow powder (0.62 g, 69%). ^{1}H NMR (400 MHz, CDCl$_3$, 25 °C) δ 6.96, 6.87 (d, 4H, Ph, $J = 9$ Hz), 4.18, 4.08 (d, 8H, Cp), 3.93 (t, 2H, OCH$_2$, $J = 6$ Hz), 3.69 (s, 4H, N-CH$_2$), 3.41 (t, 2H, BrCH$_2$, $J = 7$ Hz), 1.88 (quintet, 2H, OCH$_2$CH_2, $J = 7$ Hz), 1.76 (quintet, 2H, BrCH$_2$CH_2, $J = 7$ Hz), 1.25–1.50 (16H, –(CH$_2$)–). ^{13}C{^{1}H} NMR (100 MHz, in CDCl$_3$ at 25 °C) δ 152.4 (*ipso*, $C_6H_4OCH_2$), 145.0 (*ipso*, C_6H_4N), 117.6 (*meta*, $C_6H_4OCH_2$), 115.5 (*ortho*, $C_6H_4OCH_2$), 84.4 (N-CH$_2$), 69.9, 69.1 (Cp), 68.6 ($C_6H_4OCH_2$), 48.7 (Cp-CH_2-N), 33.9 ($C_6H_4OCH_2CH_2$), 32.8 (CH_2Br), 29.5–29.4, 28.7, 28.5, 28.2, 26.1. Anal. Calc. for $C_{30}H_{40}BrFeNO$: C, 63.62; H, 7.12; N, 2.47; Br, 14.11. Found: C, 63.30; H, 7.20; N, 2.31; Br, 14.45%.

3.6. Synthesis of N-{4-(6-mercaptohexyloxy)phenyl}-2-aza[3]ferrocenophane (1)

Thiourea (0.054 g, 0.73 mmol) was added to a dimethyl-sulfoxide solution (10 mL) of N-{4-(6-bromohexyl-oxy)phenyl}-2-aza[3]ferrocenophane (0.35 g, 0.73 mmol) and the solution was stirred at 60 °C for 24 h. A aqueous NaOH solution (3 M) was added and the mixture was stirred at 60 °C for 30 min. To the reaction mixture was added HCl aqueous solution, and the product was extracted with Et$_2$O. After drying the organic layer over Na$_2$SO$_4$, the solvent was removed by evaporation to give a yellow powder, which was purified by silica gel column chromatography (eluent = ethyl acetate: hexane = 1:1). Removal of the solvent by evaporation gave **1** as an orange solid (0.22 g, 68%). ^{1}H NMR (400 MHz, CDCl$_3$, 25 °C) δ 6.96, 6.84 (d, 4H, Ph, $J = 9$ Hz), 4.18, 4.08 (d, 8H, Cp), 3.93 (t, 2H, OCH$_2$, $J = 6$ Hz), 3.69 (s, 4H, N-CH$_2$), 2.55 (q, 2H, CH_2SH, $J = 7$ Hz), 1.77 (quintet, 2H, OCH$_2$CH_2, $J = 7$ Hz), 1.66 (quintet, 2H, CH_2CH$_2$SH, $J = 7$ Hz), 1.37 (t, 1H, SH, $J = 7$ Hz), 1.40–1.53 (4H, –(CH$_2$)–). Anal. Calc. for $C_{24}H_{29}FeNOS$: C, 66.20; H, 6.71; N, 3.22; S, 7.36. Found: C, 65.53; H, 6.88; N, 2.93; Br, 6.21%.

Other 2-aza[3]ferrocenophanes tethered to the alkanethiol **2–4** were prepared analogously and their data are shown below.

3.7. N-{4-(8-Mercaptooctyloxy)phenyl}-2-aza[3]ferrocenophane (2)

Yellow powder (0.21 g, 68%). ^{1}H NMR (400 MHz, CDCl$_3$, 25 °C) δ 6.97, 6.85 (d, 4H, Ph, $J = 9$ Hz), 4.18, 4.08 (d, 8H, Cp), 3.93 (t, 2H, OCH$_2$, $J = 6$ Hz), 3.69 (s, 4H, N-CH$_2$), 2.53 (q, 2H, CH_2SH, $J = 7$ Hz), 1.75 (quintet, 2H, OCH$_2$CH_2, $J = 7$ Hz), 1.62 (quintet, 2H, CH_2CH$_2$SH,

$J = 7$ Hz), 1.34 (t, 1H, SH, $J = 7$ Hz), 1.30–1.53 (8H, –(CH$_2$)–). ^{13}C{^{1}H} NMR (100 MHz, in CDCl$_3$ at 25 °C) δ 152.4 (*ipso*, $C_6H_4OCH_2$), 145.0 (*ipso*, C_6H_4N), 117.6 (*meta*, $C_6H_4OCH_2$), 115.3 (*ortho*, $C_6H_4OCH_2$), 84.4 (N-CH$_2$), 69.9, 68.5 (Cp), 68.5 ($C_6H_4OCH_2$), 48.7 (Cp-CH_2-N), 34.0 ($C_6H_4OCH_2CH_2$), 29.4, 29.3, 29.0, 28.3, 26.0, 24.6 (CH$_2$SH). Anal. Calc. for $C_{26}H_{33}FeNOS$: C, 67.38; H, 7.18; N, 3.02; S, 6.92. Found: C, 67.65; H, 7.24; N, 2.91; S, 6.25%.

3.8. N-{4-(10-Mercaptodecyloxy)phenyl}-2-aza[3]ferrocenophane (3)

Yellow powder (0.21 g, 58%). ^{1}H NMR (400 MHz, CDCl$_3$, 25 °C) δ 6.97, 6.85 (d, 4H, Ph, $J = 9$ Hz), 4.18, 4.08 (d, 8H, Cp), 3.93 (t, 2H, OCH$_2$, $J = 6$ Hz), 3.69 (s, 4H, N-CH$_2$), 2.53 (q, 2H, CH_2SH, $J = 7$ Hz), 1.75 (quintet, 2H, OCH$_2$CH_2, $J = 7$ Hz), 1.62 (quintet, 2H, CH_2CH$_2$SH, $J = 7$ Hz), 1.34 (t, 1H, SH, $J = 7$ Hz), 1.30–1.53 (12H, –(CH$_2$)–). ^{13}C{^{1}H} NMR (100 MHz, in CDCl$_3$ at 25 °C) δ 152.4 (*ipso*, $C_6H_4OCH_2$), 145.0 (*ipso*, C_6H_4N), 117.6 (*meta*, $C_6H_4OCH_2$), 115.5 (*ortho*, $C_6H_4OCH_2$), 84.4 (N-CH$_2$), 69.9, 68.5 (Cp), 68.5 ($C_6H_4OCH_2$), 48.7 (Cp-CH_2-N), 34.0 ($C_6H_4OCH_2CH_2$), 29.4, 29.3, 29.0, 28.3, 26.0, 24.6 (CH$_2$SH). Anal. Calc. for $C_{28}H_{37}FeNOS$: C, 68.42; H, 7.59; N, 2.85; S, 6.52. Found: C, 67.89; H, 7.72; N, 2.55; S, 6.92%.

3.9. N-{4-(12-Mercaptododecyloxy)phenyl}-2-aza[3]ferrocenophane (4)

Yellow powder (0.21 g, 56%). ^{1}H NMR (400 MHz, CDCl$_3$, 25 °C) δ 6.97, 6.85 (d, 4H, Ph, $J = 9$ Hz), 4.18, 4.08 (d, 8H, Cp), 3.93 (t, 2H, OCH$_2$, $J = 6$ Hz), 3.69 (s, 4H, N-CH$_2$), 2.53 (q, 2H, CH_2SH, $J = 7$ Hz), 1.76 (quintet, 2H, OCH$_2$CH_2, $J = 7$ Hz), 1.62 (quintet, 2H, CH_2CH$_2$SH, $J = 7$ Hz), 1.34 (t, 1H, SH, $J = 7$ Hz), 1.30–1.53 (16H, –(CH$_2$)–). ^{13}C{^{1}H} NMR (100 MHz, in CDCl$_3$ at 25 °C) δ 152.4 (*ipso*, $C_6H_4OCH_2$), 145.0 (*ipso*, C_6H_4N), 117.6 (*meta*, $C_6H_4OCH_2$), 115.5 (*ortho*, $C_6H_4OCH_2$), 84.4 (N-CH$_2$), 69.9, 69.1 (Cp), 68.6 ($C_6H_4OCH_2$), 48.7 (Cp-CH_2-N), 33.9 ($C_6H_4OCH_2CH_2$), 32.8, 29.4–29.5, 28.7, 28.5, 28.2, 26.1, 24.6 (CH$_2$SH). Anal. Calc. for $C_{30}H_{41}FeNOS$: C, 69.35; H, 7.95; N, 2.70; S, 6.17. Found: C, 69.20; H, 7.94; N, 2.56; S, 5.92%.

3.10. N-{4-(12-Dodecyloxy)phenyl}-2-aza[3]ferrocenophane disulfide (5)

10 wt% of KHCO$_3$ aqueous solution (3 mL) was added to a dichloromethane solution (2 mL) of **4**. After stirring at room temperature for 10 min under atmosphere, the product was extracted with ether. After the organic layer was dried over Na$_2$SO$_4$, the solvent was removed by evaporation to give a yellow powder, which was purified by recrystallization from dichloromethane and methanol to give **5** as a yellow powder (0.047 g, 47%). ^{1}H NMR

(400 MHz, CDCl$_3$, 25 °C) δ 6.96, 6.85 (d, 4H, Ph, $J = 9$ Hz), 4.18, 4.08 (d, 8H, Cp), 3.93 (t, 2H, OCH$_2$, $J = 6$ Hz), 3.69 (s, 4H, N-CH$_2$), 2.69 (t, 2H, CH_2S-S, $J = 7$ Hz), 1.78 (quintet, 2H, OCH$_2$CH_2, $J = 7$ Hz), 1.68 (quintet, 2H, CH_2CH$_2$S-S, $J = 7$ Hz), 1.25–1.50 (br, 16H, –(CH$_2$)–). ^{13}C{^{1}H} NMR (100 MHz, in CDCl$_3$ at 25 °C) δ 152.5 (*ipso*, C$_6$H$_4$OCH$_2$), 145.1 (*ipso*, C$_6$H$_4$N), 117.7 (*meta*, C$_6$H$_4$OCH$_2$), 115.5 (*ortho*, C$_6$H$_4$OCH$_2$), 84.4 (N-CH$_2$), 69.9, 69.2 (Cp), 68.6 (C$_6$H$_4$OCH$_2$), 48.7 (Cp-CH$_2$-N), 39.3 (CH$_2$S-S), 29.6 (C$_6$H$_4$OCH$_2$CH$_2$), 29.5, 29.4, 29.2, 28.5, 26.1.

3.11. Preparation of Au electrodes and SAMs

All experiments involved the following sequence of steps: (a) mechanical polishing and electrochemical etching [17] of a gold electrode; (b) immersion of the electrode in a MeCN solution containing 2-aza[3]ferrocenophane tethered to alkanethiol **1–4** (0.10 mM) or its disulfide **5** (0.05 mM) for 12 h; (c) rinsing with absolute MeCN followed by distilled water; (d) characterization by cyclic voltammetry in nonaqueous or aqueous electrolyte solutions. In the case of preparation of mixed SAMs, the step (b) applied as follows: (b′) immersion in a MeCN solution containing **4** (0.10 mM) or **5** (0.05 mM) and an *n*-dodecanethiol (0.10 or 1.0 mM) for 12 h. The coverages of the azaferrocenophanes were optimized by changing immersion time of the gold electrode into the MeCN solution of azaferrocenophanes. The immersion of gold electrode into the MeCN solution of **2** for 4 h provided the SAM which coverage was 5.0×10^{-11} mol cm^{-2}. The coverage of **2** was saturated by immersion of the gold electrode for 12 h to provide the SAM which coverage was 6.0×10^{-11} mol cm^{-2}. The immersion time was applied for 12 h for the preparation of SAMs.

3.12. Electron transfer rate constant

Kinetic data of electron transfer between the Fe center and the gold surface of the SAM of **2–4** were obtained with variable scanning rate from 0.02 to 12 V s^{-1}. As the scan rate is increased from 0.1 to 1.0 mV s^{-1}, these electrodes indicate quasi-reversible behavior, and the peak potential separation significantly increases above 1.0 V s^{-1}. The parameters of the separation are used to estimation of electron transfer coefficients and the symmetry factors by using Laviron's procedure [7–9], which involve following equations:

$$E_{pa} = E_a^0 - (RT/\alpha nF)\ln(RTk_a/\alpha nFv_a), \qquad (2)$$

$$E_{pc} = E_c^0 - (RT/(1-\alpha)nF)\ln(RTk_c/(1-\alpha)nFv_c). \qquad (3)$$

Here, v_a and v_c denote critical scan rates which are obtained from extrapolating the linear portion of the E_p vs. log v plots to the formal anodic and cathodic potentials E_a^0 and E_c^0 which observed at slow scan rate. The slopes of the linear portions of the E_p vs. log v curves are $-2.3RT/\alpha nF$ for the anodic branch and $2.3RT/(1-\alpha)nFv_c$ for the cathodic process. The rate constants k_a and k_c are given by $\alpha nFv_a/RT$ for the anodic process and $(1-\alpha)nFv_c/RT$ for the cathodic process, respectively.

Acknowledgements

References

[1] (a) A. Ulman, Chem. Rev. 96 (1996) 1533;
(b) R.M. Crooks, A. Ricco, Acc. Chem. Res. 31 (1998) 219;
(c) D.A. Offord, S.B. Sachs, M.S. Ennis, T.A. Eberspacher, J.H. Griffin, C.E.D. Chidsey, J.P. Collman, J. Am. Chem. Soc. 120 (1998) 4478;
(d) T. Horikoshi, M. Itoh, M. Kurihara, K. Kubo, H. Nishihara, J. Electroanal. Chem. 473 (1999) 113;
(e) T. Otsubo, Y. Aso, K. Takimiya, Bull. Chem. Soc. Jpn. 74 (2001) 1789;
(f) T. Yamada, T. Hashimoto, S. Kikushima, T. Ohtsuka, M. Nango, Langmuir 17 (2001) 4634;
(g) S.-K. Oh, L.A. Baker, R.M. Crooks, Langmuir 18 (2002) 6981;
(h) M.-C. Daniel, D. Astruc, Chem. Rev. 104 (2004) 293;
(i) J.C. Love, L.A. Estroff, J.K. Kriebel, R.G. Nuzzo, G.M. Whitesides, Chem. Rev. 105 (2005) 1103.
[2] (a) Z. Hou, N.L. Abbott, P. Stroeve, Langmuir 14 (1998) 3287;
(b) T. Kondo, S. Horiuchi, I. Yagi, S. Ye, K. Uosaki, J. Am. Chem. Soc. 121 (1999) 391;
(c) S. Kramer, R.R. Fuierer, C.B. Gorman, Chem. Rev. 103 (2003) 4367;
(d) Y.-Y. Luk, N.L. Abbott, Science 301 (2003) 623;
(e) J. Lahann, S. Mitragotri, T.-N. Tran, H. Kaido, J. Sundaram, I.S. Choi, S. Hoffer, G.A. Somorjai, R. Langer, Science 299 (2003) 371;
(f) H. Endo, T. Nakaji-Hirabayashi, S. Morokoshi, M. Gemmei-Ide, H. Kitano, Langmuir 21 (2005) 1314;
(g) F. Hapiot, S. Tilloy, E. Monflier, Chem. Rev. 106 (2006) 767;
(h) M. Haga, M. Ohta, H. Machida, M. Chikira, N. Tonegawa, Thin Solid Films 499 (2006) 201.
[3] (a) S. Zapotoczny, T. Auletta, M.R. de Jong, H. Schonherr, J. Huskens, F.C.J.M. van Veggel, D.N. Reinhoudt, G.J. Vancso, Langmuir 18 (2002) 6988;
(b) A. Anne, A. Bouchardon, J. Moiroux, J. Am. Chem. Soc. 125 (2003) 1112;
(c) Y.-T. Long, C.-Z. Li, T.C. Sutherland, M. Chahma, J.S. Lee, H.-B. Kraatz, J. Am. Chem. Soc. 125 (2003) 8724;
(d) M. Twardowski, R.G. Nuzzo, Langmuir 20 (2004) 175;
(e) T.-Y. Dong, L.-S. Chang, I.-M. Tseng, S.-J. Huang, Langmuir 20 (2004) 4471;
(f) S. Zou, Y. Ma, M.A. Hempenius, H. Schonherr, G.J. Vancso, Langmuir 20 (2004) 6278;
(g) J.P. Collman, N.K. Devaraj, C.E.D. Chidsey, Langmuir 20 (2004) 1051;
(h) R.C. Chambers, C.E. Inman, J.E. Hutchison, Langmuir 21 (2005) 4615;
(i) K. Kitagawa, T. Morita, S. Kimura, Langmuir 21 (2005) 10624.

[4] (a) C.E.D. Chidsey, C.R. Bertozzi, T.M. Putvinski, A.M. Mujsce, J. Am. Chem. Soc. 112 (1990) 4301;
(b) C.E.D. Chidsey, Science 251 (1991) 919;
(c) H.O. Finklea, D.D. Hanshew, J. Am. Chem. Soc. 114 (1992) 3173;
(d) J.F. Smalley, S.W. Feldberg, C.E.D. Chidsey, M.R. Linford, M.D. Newton, Y.-P. Liu, J. Phys. Chem. 99 (1995) 13141;
(e) K. Weber, L. Hockett, S. Creager, J. Phys. Chem. B 101 (1997) 8286.

[5] (a) S.B. Sachs, S.P. Dudek, R.P. Hsung, L.R. Sita, J.F. Smalley, M.D. Newton, S.W. Feldberg, C.E.D. Chidsey, J. Am. Chem. Soc. 119 (1997) 10563;
(b) H.D. Sikes, J.F. Smalley, S.P. Dudek, A.R. Cook, M.D. Newton, C.E.D. Chidsey, S.W. Feldberg, Science 291 (2001) 1519;
(c) S.P. Dudek, H.D. Sikes, C.E.D. Chidsey, J. Am. Chem. Soc. 123 (2001) 8033.

[6] (a) A. Togni, T. Hayashi (Eds.), Ferrocenes, VCH, New York, 1995;
(b) P. Nguyen, P. Gomez-Elipe, I. Manners, Chem. Rev. 99 (1999) 1515;
(c) T.J. Colacot, Chem. Rev. 103 (2003) 3101;
(d) D.R. van Staveren, N. Metzler-Nolte, Chem. Rev. 104 (2004) 5931, and references therein.

[7] E.J. Laviron, Electroanal. Chem. 101 (1979) 19.

[8] (a) J. Wei, H. Liu, D.E. Khoshtariya, H. Yamamoto, A. Dick, D.H. Waldeck, Angew. Chem., Int. Ed. 41 (2002) 4700;
(b) S.J. Green, N. Le-Poul, P.P. Edwards, G.J. Peacock, J. Am. Chem. Soc. 125 (2003) 3686.

[9] H.-G. Hong, T.E. Mallouk, Langmuir 7 (1991) 2362.

[10] (a) S.-I. Murahashi, K. Kondo, T. Hakata, Tetrahedron Lett. 23 (1982) 229;
(b) Y. Tsuji, K.T. Huh, Y. Ohsugi, Y. Watanabe, J. Org. Chem. 50 (1985) 1365;
(c) Y. Tsuji, K.T. Huh, Y. Yokoyama, Y. Watanabe, J. Chem. Soc., Chem. Commun. (1986) 1575.

[11] (a) I. Yamaguchi, T. Sakano, H. Ishii, K. Osakada, T. Yamamoto, J. Organomet. Chem. 584 (1999) 213;

(b) T. Sakano, M. Horie, K. Osakada, H. Nakao, Bull. Chem. Soc. Jpn. 74 (2001) 2059;
(c) K. Osakada, T. Sakano, M. Horie, Y. Suzaki, Coord. Chem. Rev. 250 (2006) 1012.

[12] (a) M. Horie, T. Sakano, K. Osakada, H. Nakao, Organometallics 23 (2004) 18;
(b) T. Sakano, M. Horie, K. Osakada, H. Nakao, Eur. J. Inorg. Chem. (2005) 644.

[13] (a) M. Horie, Y. Suzaki, K. Osakada, J. Am. Chem. Soc. 126 (2004) 3684;
(b) M. Horie, Y. Suzaki, K. Osakada, Inorg. Chem. 44 (2005) 5844.

[14] (a) F.G. Bordwell, D.L. Hughes, J. Am. Chem. Soc. 108 (1986) 7300;
(b) F.G. Bordwell, Acc. Chem. Res. 21 (1988) 456.

[15] (a) J. Alvarez, A.E. Kaifer, Organometallics 18 (1999) 5733;
(b) J. Alvarez, T. Ren, A.E. Kaifer, Organometallics 20 (2001) 3543.

[16] A.J. Bard, L.R. Faulkner (Eds.), Electrochemical Methods: Fundamentals and Applications, Wiley, New York, 1980.

[17] U. Oesch, J. Janata, Electorochim. Acta 28 (1983) 1237.

[18] P. Seiler, J.D. Dunitz, Acta Crystallogr., Sect. B B35 (1979) 1068.

[19] Y. Suzaki, M. Horie, T. Sakano, K. Osakada, J. Organomet. Chem. 691 (2006) 3403.

[20] G.K. Rowe, S.E. Creager, Langmuir 7 (1991) 2307.

[21] K. Uosaki, Y. Sato, H. Kita, Langmuir 7 (1991) 1510.

[22] (a) H.-G. Hong, W. Park, Langmuir 17 (2001) 2485;
(b) A.G. Larsen, K.V. Gothelf, Langmuir 21 (2005) 1015.

[23] (a) G.K. Rowe, S.E. Creager, J. Phys. Chem. 98 (1994) 5500;
(b) C. Barbero, M.C. Miras, E.J. Calvo, R. Kotz, O. Haas, Langmuir 18 (2002) 2756;
(c) G. Valincius, G. Niaura, B. Kazakeviciene, Z. Talaikyte, M. Kazemekaite, E. Butkus, V. Razumas, Langmuir 20 (2004) 6631.

[24] R.F. Lane, A.T. Hubbard, J. Phys. Chem. 77 (1973) 1401.

[25] (a) G. Inzelt, J. Backsai, Electrochim. Acta 37 (1992) 647;
(b) G. Inzelt, G. Horanyi, J.Q. Chambers, Electrochim. Acta 32 (1987) 757.